Xie *et al. Geoscience Letters* (2023) 10:36
https://doi.org/10.1186/s40562-023-00290-x

Geoscience Letters

RESEARCH LETTER

Preservation conditions and potential evaluation of the Longmaxi shale gas reservoir in the Changning area, southern Sichuan Basin

Weidong Xie[1,2,3], Si Chen[1,2*], Huajun Gan[1,2*], Hua Wang[1,2], Meng Wang[4] and Veerle Vandeginste[3]

Abstract

The production of shale gas varies greatly in different regions due to the way gas has accumulated and preserved. This work investigates the dynamic evolution of shale gas generation, accumulation, adjustment, and loss from the Longmaxi formation (S_1l) in the Changning area, southern Sichuan Basin, China. The factors controlling the preservation conditions and formation mechanism of the overpressure shale gas reservoir are also studied. The results show that shale gas generation reached its peak during the Middle Jurassic to Early Cretaceous. Furthermore, the gas occurs mainly in organic matter pores of nanometer size, clay mineral pores of nano- to micro-meter size, and microfractures of micrometer size. Then, in the Early Cretaceous, the reservoir was damaged due to uplift of the crust. Additionally, the evaluation scheme of the shale gas reservoirs is established according to the organic geochemical parameters, mineralogical composition, sealing capacity, thickness, burial depth, faults, pressure coefficient, and gas content, etc. Hence, the shale gas reservoirs may be divided into four grades, with Class I being the grade with best gas preservation and Non-economic grade with the worst gas preservation. The annular region in the Jianwu–Luochang synclines and the northeast limb of the Changning anticline have optimum preservation conditions, with a grade of Class I. The preservation conditions gradually deteriorate towards the two limbs, with Class II, Class III, and Non-economic area grades. The good preservation conditions correspond to a high pressure coefficient, and the pressure of the reservoir is mainly caused by hydrocarbon generation pressurization of organic matter (mainly the stage of oil cracking gas and dry gas), tectonic uplift pressurization, and to a minor extent, transformation dehydration pressurization of clay minerals. Furthermore, overpressure preservation is controlled by microporous overpressure, source rock–caprock vertical sealing ability, the spatial distribution of S_1l, and development characteristics of faults. Results from this investigation provide specific guidance for shale gas exploitation in the study area, and provide a reference for the evaluation of preservation conditions in shale gas reservoirs and formation mechanism of overpressure gas reservoirs.

Keywords Shale gas, Reservoir evolution, Preservation condition, Overpressure mechanism, Southern Sichuan Basin

*Correspondence:
Si Chen
sichen720@hotmail.com
Huajun Gan
hjgan@cug.edu.cn
Full list of author information is available at the end of the article

Introduction

Recognized as a crucial unconventional resource, shale gas reservoirs are undergoing large-scale exploration and development on a global scale, and the investigation of the accumulation mechanism and preservation conditions before exploration is critical (Freeman et al. 2011; Kirk et al. 2012; Ma et al. 2020a). The accumulation mechanism of shale gas is mostly discussed from the perspective of shale gas generation and accumulation. Hence, the hydrocarbon generation history and accumulation sites have been reconstructed and characterized accordingly, leading to the qualitative to semi-quantitative characterization of hydrocarbon generation stages, types and enrichment characteristics (Jarvie et al. 2007; Hill et al. 2007; Tang 2018; Xie et al. 2022a). After gas accumulation, the preservation condition changes and deteriorates because of subsequent tectonic movement, involving changes in burial depth, continuity and spatial distribution of the reservoir, development of faults and folds, thickness and integrity of caprocks (Tu et al. 2014; Zou et al. 2016; Wilson et al. 2016; Yasin et al. 2021), etc. Consequently, the gas content and production may vary in different shale gas wells, corresponding to different reservoir quality. Based on these factors, previous studies evaluated the reservoir quality from the aspects of hydrocarbon generation potential (mainly through organic matter content and maturity) (Rashid et al. 2020; Ahmad et al. 2021), engineering conditions of reservoir stimulation (mainly through the ratio of clay content and brittle mineral content) (Ibrahim Mohamed et al. 2019), continuity and spatial distribution of reservoirs (Yu et al. 2014; Moridis and Reagan 2021), sealing capacity of caprocks (mainly including lithology, continuity, porosity and permeability) (Li et al. 2020; Ukaomah et al. 2021), the development of geological structure (mainly including faults and folds) (Shoieb et al. 2020), pressure coefficient and gas content of reservoirs (Liu et al. 2012; Guo 2016), etc. However, an integrated quantitative evaluation scheme covering the above indexes is still lacking.

Based on previous studies, the pressure coefficient is considered a crucial parameter which could represent comprehensive preservation conditions of shale gas reservoirs (Zou et al. 2016; Han et al. 2016). Therefore, it is vital to determine the formation origin and mechanism of overpressured reservoirs. Liu et al. (2020) explored the pressure coefficient based on fluid inclusion analyses, drilling data, and core microscopic observations and indicated that the overpressure is caused by hydrocarbon generation, transformation of clay minerals, and the sealing of high-quality caprocks and faults. Gao et al. (2019) stated that hydrocarbon generation is the primary origin of reservoir overpressure, especially dry gas generation. After gas accumulation, the pressure coefficient gradually decreases due to crustal uplift, caprock erosion, and structural transformation (Dong et al. 2018; Akrout et al. 2021). Hence, it is indispensable to reveal the influence of the thermal evolution and hydrocarbon history of source rock and the geological structural conditions on overpressure generation, evolution and preservation.

This work concentrates on a study area located in the southern Sichuan Basin, with shale gas that is commercially explored. However, the gas production varies significantly, which is caused by the difference in reservoir quality. Generally, the tectonic uplift of the Sichuan Basin is considerable, the structure of the southern Sichuan Basin is complex, and the tectonic uplift difference after the last hydrocarbon generation peak of the Longmaxi shale is considerable, resulting in the production difference (Rodrigues and Goldberg 2014; Chen 2014; Liao 2019). However, a quantitative evaluation of the reservoir quality has rarely been investigated. Based on the challenges mentioned above, the sedimentary burial history, thermal evolution and hydrocarbon generation history of the Longmaxi shale is reconstructed using PETROMOD 2012 (an oil and gas system simulation software, developed by IES company, Germany); the gas accumulation space is characterized using Field Emission Scanning Electron Microscopy and Low-temperature N_2 and CO_2 adsorption experiments; The evaluation scheme of the reservoir quality is established according to the organic geochemical properties, mineralogical composition, spatial distribution, geological structure, pressure coefficient, gas content, etc. Furthermore, the reservoir is divided into different grades. Finally, the geological model of gas generation, accumulation, adjustment, loss, and overpressure evolution is established through time according to the factors mentioned above. The results from this work are of great significance to establish an evaluation scheme, and to gain crucial insights beneficial for the exploration of shale gas in the southern Sichuan Basin.

Investigation, experiments and methodology

Geological background

The study area is located in the southern Sichuan Basin. Specifically, this region lies along the southern edge of the southwestern Sichuan low and gentle fold belt, which is the junction of the south Sichuan fold belt and Loushan fault-fold belt (Fig. 1). The large folds in the study area control the surface structural features, including the Changning anticline, Luochang syncline, and Jianwu syncline from north to south. The Changning anticline was initially uplifted in the Early Yanshanian and gradually raised in the Late Yanshanian. The anticline widened continuously, and the widened Luochang syncline and Jianwu syncline formed in the Early Himalayan

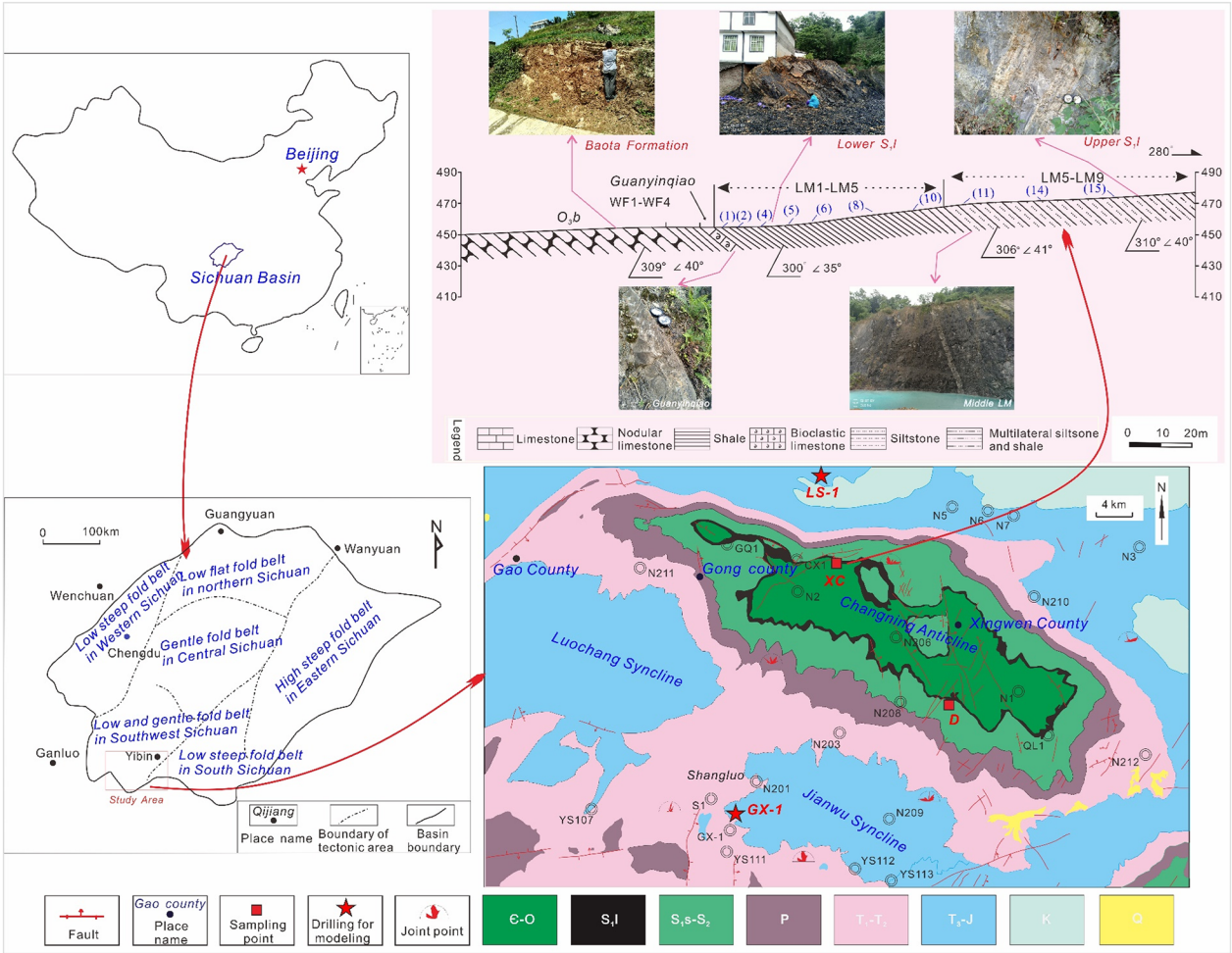

Fig. 1 Location of the study area and distribution of investigation sites. WF1–WF4 refers to the four intervals of the Wufeng formation, LM1–LM9 refers to the nine intervals of the Longmaxi formation, O_2b is the Baota formation of the Middle Ordovician, S_1l is the Longmaxi formation of the Lower Silurian, S_1s–S_2 is the Shiniulan and Hanjiadian formations of the Lower to Middle Silurian. Samples XC-1-XC-15 and D1–D7 are collected from the sampling points of series XC and D, respectively

(He et al. 2019a). The Changning anticline starts from the west of Xuyong County in the east, ends in Gaoxian County in the west, and its axis has a NW–SE direction. The anticline is wide in the east and narrow in the west. Cambrian and Ordovician formations are exposed in the core of the anticline, and Silurian, Permian, Triassic, Jurassic, and Cretaceous formations are exposed in the two limbs. Upper Triassic or Jurassic layers are exposed in the core of the Luochang and Jianwu synclines, and older strata occur in the limb outcrops. Additionally, the faults are widely developed in the core of Changning anticline, and the faults cut and intersect each other, which is characterized by multi-stage superposition. In contrast, regional faults of the Luochang and Jianwu synclines developed poorly (Fig. 1). In terms of lithology, the Cambrian strata consist of the Gaotai and Loushanguan formations, composed of siltstone, dolomitic limestone, and dolomite. The Ordovician strata overlie the Cambrian strata with a conformable contact, and are the Tongzi, Honghuayuan, Meitan, Shizipu, and Baota formations consist of dolomitic limestone and limestone, whereas the Wufeng formation is dominated by bioclastic limestone and organic rich shale. The Silurian strata also show a conformable contact with the underlying strata, and the Longmaxi formation mainly comprises organic rich shale, whereas the Shiniulan and Hanjiadian formations contain limestone, mudstone, and sandstone. Upper Silurian, Devonian, and Carboniferous formations are absent in the study area, and there is a disconformity between Permian and Silurian strata. Sediments include thin coal seam, mudstone, siltstone, and bioclastic limestone. Triassic strata show a conformable contact with

Permian strata, and the lithology is mainly composed of limestone, mudstone, and sandstone. Jurassic and Cretaceous strata are a set of clastic sediments, and only partially developed in the study area.

The investigation in the field involves the observation of the exposed strata, outcrop profiles measurement, sample collection of the Longmaxi shale, and joint points measurement. Cambrian–Quaternary strata are exposed in the study area, whereas the Devonian and Carboniferous strata are missing. The profile measurement includes the lithology, paleobiology, and thickness of the Longmaxi shale, overlying, and underlying strata. Samples of the Longmaxi shale are collected from two high-quality profiles. For example, the XC profile is an outcrop located at the core of the Changning anticline (Fig. 1). Ten shale samples are collected from this profile, weathered samples on the surface are removed and fresh samples are selected during the collection process. They are immediately stored in a sealed bag and sent to the laboratory for subsequent experiments. Samples XC-1 to XC-15 represent the shale from the bottom to the top of the Longmaxi formation. Note that sampling was not conducted over equal intervals due to the diversity and heterogeneity of Longmaxi shale. The lower part (LM1–LM5) is deposited in a deep-water shelf facies environment, with the characteristics of high organic matter content (TOC), gas content, and exploitation potential (Dong et al. 2018; Liang 2018). Carbonaceous shale and siliceous shale are the main compositions. In contrast, it changes to a shallow-water shelf facies for the deposition of the upper part (LM5–LM9), and the TOC, gas content, and exploitation potential are lower correspondingly (Dong et al. 2018; Liang 2018). Siltstone and calcareous shale are dominant. Consequently, sampling intervals of the lower part are small (< 10 m), and more samples are collected; whereas more than 10 m intervals are set for the upper part (Fig. 1). Over 160 joint points are measured, composed of the Longmaxi formation, the Longtan formation of Upper Permian, the Feixianguan, Jialingjiang, and Xujiahe formations of the Triassic, and the Ziliujing formation of Lower Jurassic. The Longmaxi shale is mainly a set of shallow–deepwater shelf facies sedimentary products composed of dark gray–black carbonaceous shale, siliceous shale, silty shale, and argillaceous siltstone (Luo et al. 2016).

Experimental procedure

The organic geochemical parameters, mineralogical composition, porosity and permeability, and pore structure parameters are obtained by experimental tests. Specifically, the TOC is determined by conducting CS-300 high-frequency infrared carbon sulfur analyzer tests, thermal maturity (R_o) is measured by conducting Axio Scope. A1A Pol & MSP 200 microphotometer tests and the mineralogical composition is determined using an X'pert powder X-ray diffractometer. The porosity and permeability are tested using an Autopore 9500 automatic mercury porosimeter. Autopore 9500 automatic mercury porosimeter and Tristar 3020 specific surface physical adsorption instruments (low-temperature N_2 and CO_2 adsorption experiments) are utilized to measure the pore volume and specific surface area. The pores in shale are divided into micropores (< 2 nm), mesopores (2–50 nm), and macropores (> 50 nm) according to the IUPAC (International Union of Pure and Applied Chemistry) classification (Rouquerol et al. 1994). The pore structure parameters are selected from the low-pressure CO_2 adsorption results with a pore size less than 1.5 nm, low-pressure N_2 adsorption results with the pore size ranging from 1.5 nm to 50 nm, and high-pressure mercury injection results with a pore size higher than 50 nm. The results are presented in Tables 1 and 2. The TOC of samples ranges from 1.69 to 9.73%, with an average of 3.94%. R_o is in the range of 2.35 to 2.84%, which is in the over maturity stage. Both TOC and R_o of the Longmaxi shale in the study area meet the standard of high-quality reservoir (TOC > 2.0 and R_o > 2.0), which indicates that a large amount of hydrocarbons are generated during the geological history (Tu et al. 2014; Zou et al. 2016). However, the performance of porosity and permeability is worse, which is generally characterized by low porosity and ultra-low permeability (Chen et al. 2018; Tang et al. 2019). The former is in the range of 4.9–8.56% (6.47% on average), and the latter ranges from 0.00036 to 0.0086 mD (0.0023 mD on average). Hence, fracturing stimulation is necessary to improve porosity, permeability, and gas recovery. For a better three-dimensional fracture network and high-quality reservoir, the brittle mineral content should higher than 40% (Li 2012; Jiang et al. 2020). It ranges from 79 to 92% (85.6% on average) in this study, and mainly comprises quartz, carbonate and feldspar (Table 1). The clay mineral content is in the range of 8 to 21% (14.3% on average), and it contains mainly of illite and mixed I/S.

Reconstruction method of sedimentary burial, thermal evolution, and hydrocarbon generation history

Restoration of erosion thickness and basin simulation parameters

The acoustic transit time (Magara 1981) and strata trend thickness are employed to calculate the erosion thickness of the overlying strata of the Longmaxi formation. From this analysis, the erosion thickness of the Triassic and overlying strata is greater than the sediment thickness, and it can be concluded that the pores of the rocks were not subjected to secondary compaction during

Table 1 The organic geochemical parameters, mineral composition, porosity, and permeability of shale samples

Sample ID	TOC (%)	R_o (%)	Porosity (%)	Permeability (mD)	Mineral composition (%)						
					Quartz	Feldspar	Calcite	Dolomite	Pyrite	Clay	TCBM
XC-1	9.73		8.56	0.00129	74	5		3		18	82
XC-2			4.65	0.0086							
XC-4	4.46		6.11	0.00011	69	5	12	6		8	92
XC-5	3.6				37	2	23	29		9	91
XC-6	3.13				38	5	21	25		11	89
XC-8	4.03		7.63	0.00036	39	4	24	22		11	89
XC-10	5.55		6.98	0.00168	31	5	11	42		11	89
XC-11	1.69				36	20	11	12		21	79
XC-14	4.28				62	8	5	9	2	14	86
XC-15	3.49		4.9	0.00159	73	13				14	86
D1	4.96	2.35			54	13	6	3	5	19	81
D2	4.89	2.46			50	17	6	6	4	17	83
D3	2.98	2.28			46	22	6	5	3	18	82
D4	2.09	2.81			47	25	5	4	2	17	83
D5	1.83	2.84			46	31	5	3	1	14	86
D7	2.33	2.61			43	33	6	3	1	14	86

TOC is total organic carbon, R_o is the vitrinite reflectance, and TCBM is the total content of brittle minerals

Table 2 The relative content of clay minerals

Sample ID	Relative content of clay minerals (%)		
	I/S	Illite	Chlorite
XC-1	20.0	78.0	2.0
XC-4	24.0	76.0	
XC-5	19.0	79.0	2.0
XC-6	25.0	75.0	
XC-8	19.0	81.0	
XC-10	20.0	80.0	
XC-11	24.0	60.0	16.0
XC-14	21.0	74.0	5.0
XC-15	22.0	78.0	

sedimentation. The acoustic transit time (Eq. 1) applies to the restoration of erosion thickness in this period. In contrast, the erosion thickness of Devonian, Carboniferous, and Permian is less than the overlying sediments, so that the rock pores are subject to secondary compaction during sedimentation. As a result, the acoustic transit time is no longer applicable, so the strata trend thickness is employed to restore their erosion thickness. The restoration results of the erosion thickness are depicted in Additional file 1: Table S1.

$$\Delta t = \Delta t_0 e^{-CH}, \tag{1}$$

where H is the burial depth (m); Δt is the transit time of shale at depth H (μs/m); Δt_0 is the surface transit time (μs/m); C is the trend slope of the strata normal compaction (m^{-1}).

Additionally, the boundary conditions (paleo-water depth, sediment–water interface temperature, and heat flow) are required to restore the thermal evolution history. The boundary conditions are based on previous research results (Additional file 1: Table S2) of the Well LS-1 and Profile XC (Jiang et al. 2015; Tang 2018). Jiang et al. (2015) and Tang (2018) measured the paleo-water depth, sediment–water interface temperature, and heat flow of the southern Sichuan Basin based on the data of Well LS-1, H-1, W-28, YS-2, Y-14, and XC profile. Among them, Well LS-1 is located on the north edge of the study area and XC profile is located at the core of Changning anticline (Fig. 1); hence, they could represent the boundary conditions of the restoration of erosion thickness in the study area.

Reconstruction procedures of sedimentary burial, thermal evolution, and hydrocarbon generation history

The PetroMod 2012 1D module is used for the reconstruction process, consisting of input, simulation, and output units. The input involves main input and boundary conditions. Firstly, input is required on the information of strata, top and bottom depth of stratum, present thickness, eroded thickness, deposition age, erosion age, lithology (Additional file 1: Table S1), and source rock parameters (TOC is the average content of the lower Longmaxi shale, kinetics, and HI refer to the result of Tang (2018) for main input). Secondly, input is needed

on the paleo-water depth, sediment–water interface temperature, and heat flow for the boundary conditions (Additional file 1: Table S2). Then, the simulation is run and results are obtained. The burial depth, temperature, and vitrinite reflectance are presented using default plots.

Evaluation of fault complexity and reservoir grade

Evaluation of fault complexity

To accurately reflect the intensity of the faults, the study area is divided into several equal grids distributed horizontally and vertically, and these are numbered. The determination of grid size is based on the extensive fracture scale and the scope of the study area. The zoning significance is limited if the grid is too large. Correspondingly, the practical significance is meaningless if the grid is too small. The number of faults is counted in each grid, the data serve as input along with the corresponding grid coordinate points for MATLAB, and the fault complexity is classified according to the method of Natural Breaks [A method of grid data segmentation, widely used in spatial data classification (Chen et al. 2013)]. Furthermore, quantitative evaluation contours are obtained using the visualization function module in MATLAB.

Evaluation of reservoir grade

The classification criteria of gas reservoir grade and development potential include preservation conditions, hydraulic fracturing conditions, construction difficulty, etc. Specifically, it is a comprehensive vertical superposition of TOC, R_o, clay and brittle mineral content, sedimentary burial, thermal evaluation and hydrocarbon generation history, thickness, burial depth, caprocks, fault complexity, pressure coefficient, and gas content, etc. The drawing of burial depth and thickness contours of the Longmaxi shale is based on the logging-well data of drillings in the study area. The drawing of gas content and pressure coefficient contours are also based on the logging-well data of drillings as well as previous research results. It should be noted that the evaluation scheme and drawing of a reservoir classification evaluation map may have a certain subjectivity, and this is mitigated by the experience in classification based on previously obtained research results.

Results and discussion

Maturation of organic matter and gas generation

The Longmaxi shale is characterized as organic-rich and high over mature (Table 1), which indicates that large-scale oil and gas formed during its geological history. The process of shale gas generation and accumulation is reconstructed by the sedimentary burial, thermal evolution, and hydrocarbon generation history of source rock (Figs. 2, 3).

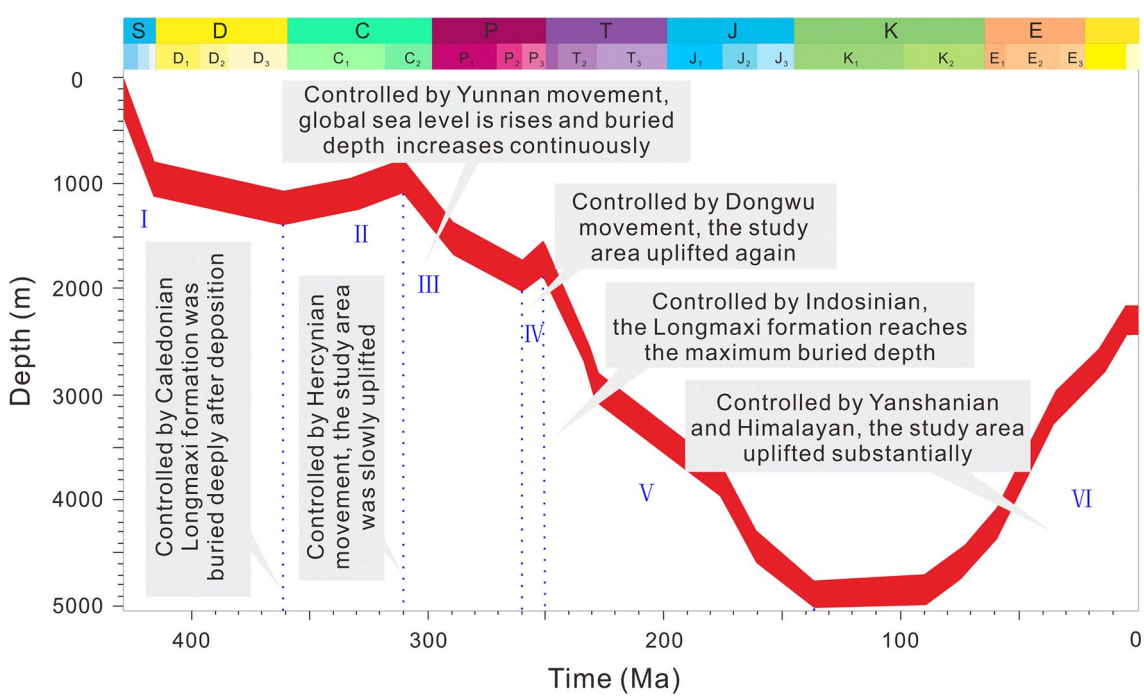

Fig. 2 Sedimentary burial history of the Longmaxi shale in Well GX-1. S is the Silurian; D, P, T, J and E are the Devonian, Permian, Triassic, Jurassic, and Paleogene, and the subscript 1, 2, and 3 represent the lower, middle and upper parts, respectively; C and K are the Carboniferous and Cretaceous, and the subscript 1, 2 represent the lower and upper parts, respectively

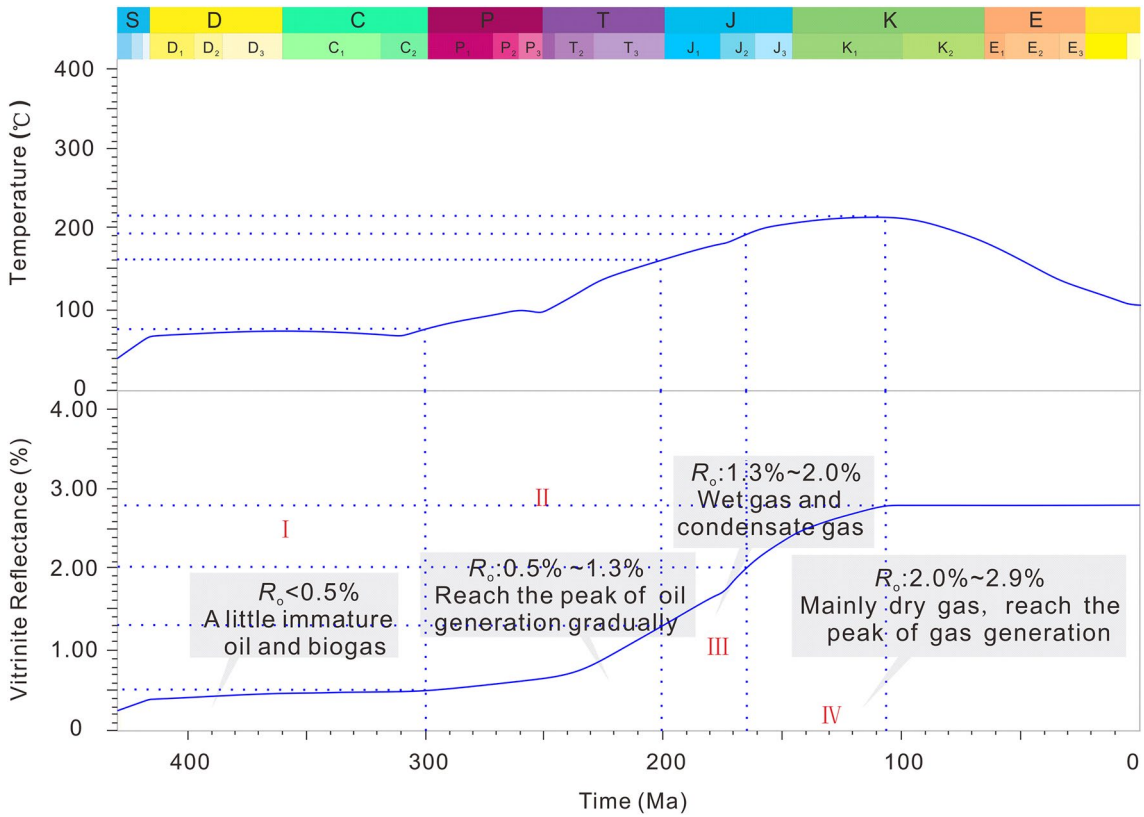

Fig. 3 Thermal evolution and hydrocarbon generation history of the Longmaxi shale in Well GX-1. S is the Silurian; D, P, T, J and E are the Devonian, Permian, Triassic, Jurassic, and Paleogene, and the subscript 1, 2, and 3 represent the lower, middle and upper parts, respectively; C and K are the Carboniferous and Cretaceous, and the subscript 1, 2 represent the lower and upper parts, respectively

(i) Before late Carboniferous time, the sedimentary evolution of the Longmaxi shale was controlled by Caledonian movement (the burial depth of Longmaxi shale increased continually) and Liujiang movement of the Hercynian (the burial depth of Longmaxi shale uplifted slowly), the strata temperature increased slowly, and the thermal maturity of organic matter was lower than 0.5%. The organic matter was immature in this stage, and the evolution of organic matter was dominated by biochemical action. The structure of organic matter consisted mostly of straight-chain alkanes, with fewer polycyclic aromatic hydrocarbons, simultaneously, aromatization began. As a result, a low amount of biogas and immature oil were generated in this process. (ii) From the Upper Carboniferous to the end of the Triassic, the sedimentary evolution of the Longmaxi shale was controlled by the Yunnan and Dongwu movements of the Hercynian and Indosinian. The burial depth of the Longmaxi shale increased continually, and the strata temperature and R_o (0.5–1.3%) increased rapidly. The organic matter evolved into the mature stage and converted to the "liquid window" dominated by aromatization and cyclocondensation. Simultaneously, thermal cracking began, the amount of saturated straight-chain alkanes decreased, whereas the amount of cycloalkanes and polycyclic aromatic hydrocarbons increased. The main products were oil and wet gas at this stage. (iii) From the end of the Triassic to the Middle Jurassic, the sedimentary evolution of the Longmaxi shale was controlled by Indosinian, and thus, the burial depth, temperature, and thermal maturity (1.3–2.0%) increased rapidly. The evolution of organic matter was dominated by thermal cracking, beyond the limit of oil generation. The products were mainly wet gas and condensate gas at this stage. (iv) From the Middle Jurassic to the Early Cretaceous, the sedimentary evolution of the Longmaxi shale was controlled by Indosinian, and thus, the burial depth, temperature, and thermal maturity (2.0–2.9%) kept increasing. The evolution of organic matter was dominated by thermal cracking and a large amount of pyrolysis gas was generated, which reached the gas generation peak.

Characteristics of shale gas accumulation sites

Morphology of shale pores

Source rock is also the reservoir rock for shale gas reservoirs, and in situ accumulation or short-distance

migration occurs in the pores and microfractures. Consequently, characteristics of the reservoir space control gas content. The pore types in shale are divided into organic matter pores, intergranular pores, intragranular pores, and microfractures (Loucks et al. 2012). Moreover, the morphological types can be further divided according to the developmental sites. Hydrocarbon generation pores in organic matter, interlayer pores and intergranular pores in clay minerals, dissolution pores and intergranular pores of brittle minerals, and microfractures are observed in the shale samples (Fig. 4). The pore size of brittle mineral pores and microfractures is mostly at micro-scale, clay mineral pores are mostly at micro–nano scale, and organic pores are mainly at nano-scale.

Quantitative characterization of pore structure parameters

Pore volume (PV) and specific surface area (SSA) are the crucial evaluation parameters of shale reservoir, which provides the accumulation space and adsorption sites (Wang et al. 2019; Xie et al. 2021). The pore size distribution curves are characterized by mercury injection, low-pressure N_2, and low-pressure CO_2 adsorption experiments. The PV curves are multi-modal, and the dominant pore size ranges are distinct in different shale samples (Fig. 5a). It is mainly micropores and mesopores that contribute to the PV of samples D1, D2, and D3 (the bottom of the Longmaxi formation), whereas there are relatively few macropores. Micropores, mesopores, and macropores all contribute significantly to the PV of samples D4, D5, and D7 (the middle–lower of the Longmaxi formation). In comparison, micropores dominate the SSA in all shale samples, mesopores follow, and the contribution of macropores is negligible (Fig. 5b).

Adjustment, loss, preservation conditions, and quality evaluation of shale gas reservoir

Evaluation scheme

Since the Early Cretaceous, the uplift of the southern Sichuan Basin was substantially controlled by the Middle–Late Yanshanian and the subsequent Himalayan movement, and the burial depth and strata temperature of the Longmaxi shale kept decreasing, leading to the end of hydrocarbon generation. Correspondingly, the Longmaxi shale gas reservoir evolved to the stage of adjustment and loss, which includes the changes in gas occurrence state caused by shallower burial depth, weakening of the sealing ability of overlying strata to the gas reservoir caused by erosion, and gas loss caused by the transformation of the geological structure. Consequently, the preservation conditions in the study area are diverse, and the quality grade and exploitation potential of gas reservoirs are correspondingly different. Therefore, the evaluation scheme of exploitation potential is established by comprehensively considering the hydrocarbon generation potential of source rock, fracturing engineering conditions, reservoir continuity and spatial distribution, the self-sealing ability of shale reservoir, the sealing ability of roof, floor, and regional caprocks, the development of faults and folds, pressure coefficient, and gas content (Table 3). Some threshold value of evaluation parameters refers to Li (2012), Tu et al. (2014), Zou et al. (2016), Jiang et al. (2020), Ma et al. (2020b), and Ge et al. (2021). Then, the shale gas reservoirs in the study area are divided into four grades. The Non-economic class represents reservoirs with characteristics of shallow burial depth, close to erosion areas of the Longmaxi shale, poor continuity, deteriorated by deep and large faults, low pressure coefficient, and low gas content. Class I represents reservoirs with excellent gas preservation conditions and development engineering conditions. Class II represents reservoirs with good gas preservation conditions and development engineering conditions. Finally, Class III represents reservoirs with excellent gas preservation conditions, but with too high engineering difficulty of development.

Gas generation potential and engineering conditions

The gas generation potential is evaluated by the organic geochemical parameters (TOC and R_o). The test results in this work (with an average TOC of 4.44% and an average R_o of 2.45% in Table 1) and the test results of Zeng (2011), Yang (2016), and Chen (2018) (the average TOC of the entire study area is higher than 2.0% and increases from southeast to northwest, and the average R_o of the entire study area is higher than 2.0% and increases from southeast to northwest in the study area) meet the conditions of Class I shale gas reservoirs (Table 3). Engineering conditions comprise reservoir continuity, burial depth, clay content, and brittle mineral content of the reservoir. The average clay content (14.4%) and brittle mineral content (85.6%) in this work (Table 1) meet the characteristics of Class I shale gas reservoirs, and Jin et al. (2014) and Xu et al. (2021) also reported a similar conclusion for shale samples in the lower part of the Longmaxi formation. The thickness and burial depth of Longmaxi shale are clearly distinct in the study area (Fig. 6a, b). The thickness of an exploitable gas reservoir should be greater than 30 m (Li 2012; Li et al. 2016). The total thickness of the Longmaxi shale is mainly in the range of 200–400 m with excellent continuity. The thickness increases in the NE direction (Fig. 6a). Moreover, the burial depth of the reservoir affects shale gas exploration and development. The depth range of 1000–6000 m represents the exploratory shale gas reservoir. The regional caprocks would be eroded if the burial depth was too shallow,

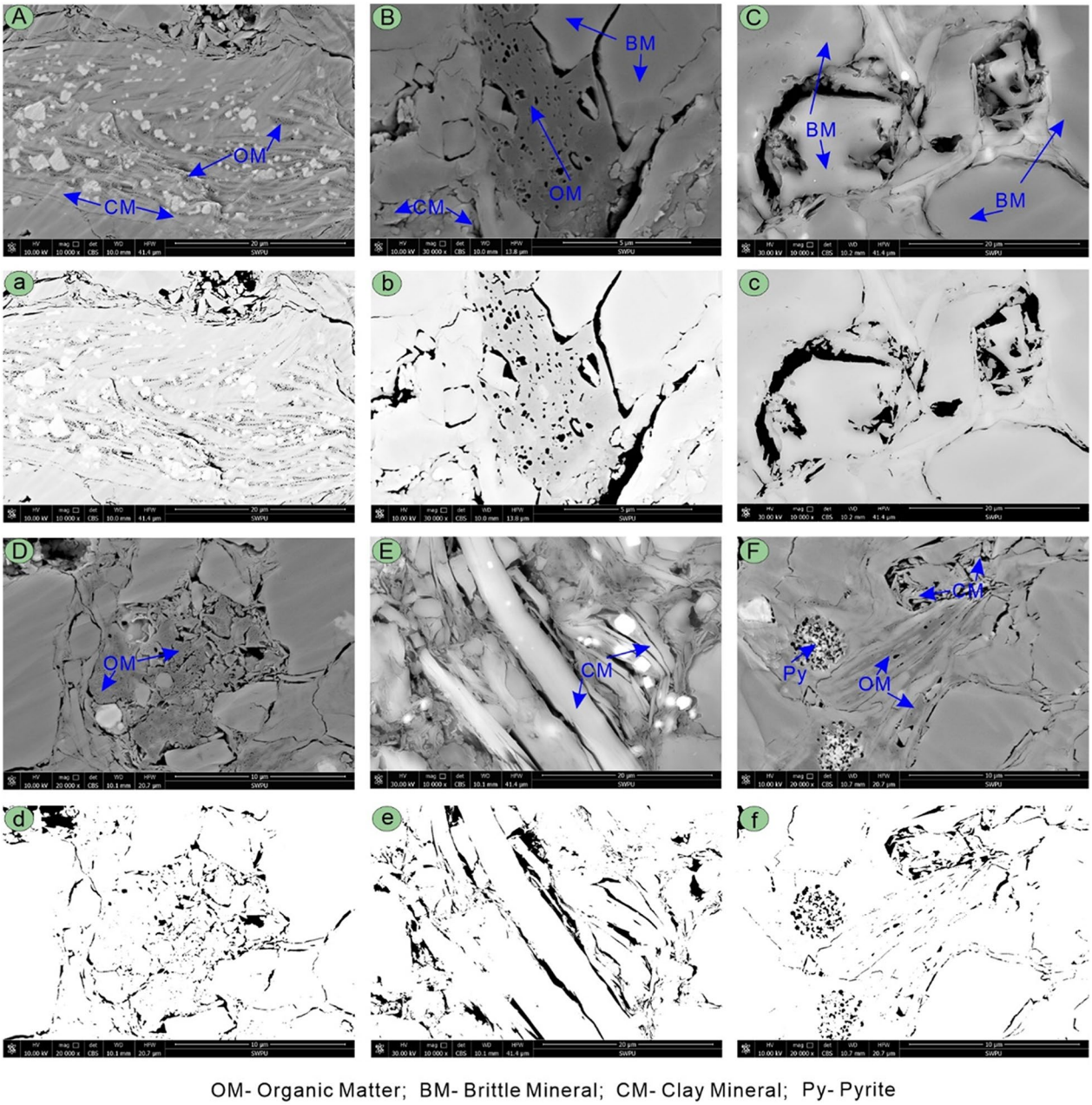

Fig. 4 Pores in SEM images of the Longmaxi shale samples. **A**: XC-1, the bottom of the S_1l, black carbonaceous shale, organic matter is distributed among clay minerals, hydrocarbon generation pores developed; **B**: XC-6, the lower part of the S_1l, black siliceous shale, organic matter pores, and microfractures developed; **C**: XC-1, the bottom of the S_1l, black carbonaceous shale, dissolution pores, and microfractures developed; **D**: XC-5, the lower part of the S_1l, black siliceous shale, organic matter pores, microfractures, and intergranular pores developed; **E**: XC-4, the lower part of the S_1l, black siliceous shale, interlayer pores, stacked pores, and interlayer microfractures developed; **F**: XC-4, the lower part of the S_1l, black siliceous shale, pyrite mold pores, interlayer pores of clay minerals, and microfractures developed, and a certain amount of organic pores are filled with clay minerals. **A**–**F** are SEM images of shale samples, and a–f are the extraction of pores from images **A**–**F** correspondingly

resulting in poor preservation conditions. At the same time, the development difficulty and cost are extremely high when the burial depth is greater than 3500 m. A burial depth of 1500–3000 m is associated with moderate development difficulty and good preservation conditions. At the core of the Changning anticline, there is an erosion area of the Longmaxi shale, and the burial depth gradually increases to both limbs. The maximum burial depth in the northeast corner of the study area is greater than 3500 m. The core of the

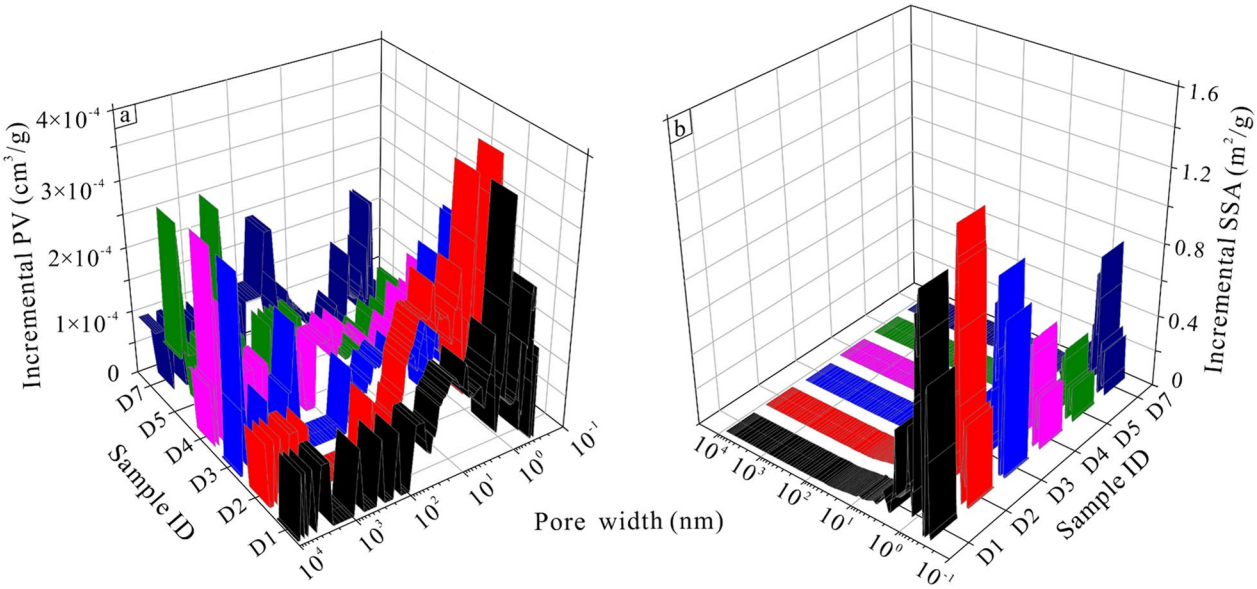

Fig. 5 Pore size distribution versus the pore volume (**a**) and pore specific surface area (**b**)

Table 3 The evaluation scheme of exploitation potential for shale gas reservoirs

Evaluation index	Reservoir grade			
	Non-economic	Class I	Class II	Class III
TOC (%)	< 0.5	> 2.0	1.0–2.0	0.5–1.0
R_o (%)	< 1.0 or > 4.0	2.0–3.5	1.0–2.0	3.5–4.0
Brittle mineral content (%)	< 15	> 40	40–30	30–15
Clay mineral content (%)	> 40	< 20	20–30	30–40
Thickness (m)	< 30	> 200	100–200	30–100
Burial depth (m)	< 1000	1000–3000	3000–4500	> 4500
Geological structural conditions	Extremely complex, close to erosion area or deep fault	Simple	Relatively complex	Complex
Pressure coefficient	< 1.0	> 2.0	1.5–2.0	1.0–1.5
Gas content (cm^3/g)	< 1.0	> 2.0	1.5–2.0	1.0–1.5

Jianwu and Luochang synclines is buried more than 3000 m, and the burial depth is gradually shallower to the south (Fig. 6b).

On the other hand, the burial depth of the Longmaxi gas reservoir also affects the erosion of the overlying strata and controls the distribution characteristics of regional caprocks. As mentioned earlier, the exposed strata include Cambrian to Cretaceous strata in the study area and affected by the amplitude of uplift (Fig. 1), which indicates a clear difference in erosion thickness. In general, there are two sets of high-quality caprocks in the study area (Fig. 7):

(i) The Shiniulan–Hanjiadian formations ($S_1s + S_2h$) of the Lower Silurian are direct caprocks of the Longmaxi reservoir. Argillaceous limestone, limestone, sandstone, and mudstone comprise this set of strata with a thickness greater than 650 m. He et al. (2019b) reported that the strong sealing capacity of the Shiniulan and Hanjiadian formations (average porosity, permeability, and breakthrough pressure of 0.59%, 0.0026 mD, and 76.1 MPa, respectively) is a significant reason for the preservation of the Longmaxi shale gas reservoir, supplemented by an argillaceous limestone sealing layer of the underlying Baota formation (O_2b) (average porosity, permeability, and breakthrough pressure of 1.5%, 0.013 mD, and 67.8 MPa, respectively). This set of strata is widely distributed in the study area, except for the sedimentary absence in the core of the Changning anticline.

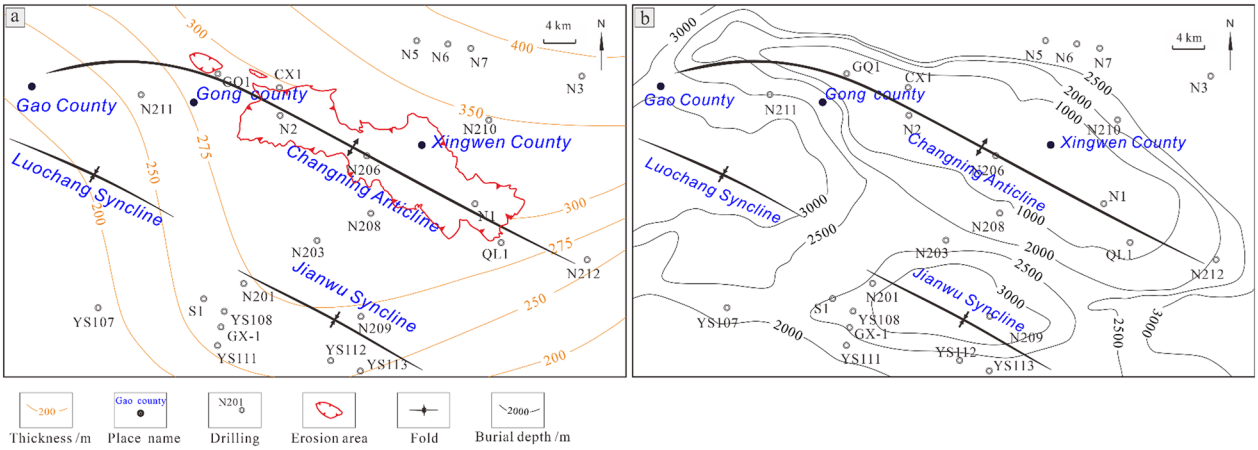

Fig. 6 Thickness and burial depth of the Longmaxi shale in the study area. **a** is thickness contour map, and **b** is burial depth contour map

(ii) The Jialingjiang formation (T_1j) of the Lower Triassic is the optimum regional caprock (porosity < 10% and permeability < 1 mD), which is a set of marine limestone, dolomite, and gypsum with a thickness of 400–600 m in southern Sichuan Basin. Certain areas are eroded and result in the sedimentary absence of T_1j in the study area, the thickness in Well GX-1 is eroded to about 100 m. Its distribution has clear regional characteristics. T_1j is well preserved in the Luochang and Jianwu synclines' core and the north of the study area. In contrast, it is not developed in the core of the Changning anticline and the south of the study area. Additionally, the Middle Permian strata have also a certain sealing ability. However, those strata are not deemed a high-quality caprock due to the lithological changes affected by the Emeishan basalt in the study area.

Structural characteristics and its damage on reservoir and caprocks

The Longmaxi reservoir experiences an uplift and it comes into the adjustment stage after the last peak of hydrocarbon generation (Early Cretaceous). The gas reservoir is affected by geological structures, meaning faults and folds formed and impacted the reservoir, underlying strata, and caprocks, resulting in the deterioration of the preservation conditions of the gas reservoir. The occurrence of the faults is similar to the results of joint points, mainly spreading along NW–SE and NE–SW directions (Figs. 8, 9). Referring to the tectonic evolution history of the Sichuan Basin (He et al. 2019a), the NE–SW trending joints are consistent with the tectonic stress field of the Early–Middle Yanshanian. The NW–SE trending joints are consistent with the tectonic stress field of the Late Yanshanian.

Additionally, fault intensity is quantitatively graded in the study area based on the number of faults and their intersections per unit area. As illustrated in the quantitative evaluation results (Fig. 8), faults developed mostly in the Changning anticline, especially the eastern part of the anticline core, which is divided into complex and transitional areas. The faults provide migration channels for shale gas loss and worsen the preservation condition of the reservoir. In contrast, the Jianwu and Luochang synclines and the northeast of the study area are simple and stable areas. Those regions are mainly syncline or monocline with wide and gentle characteristics, and faults developed poorly. Hence, gas diffusion and loss are relatively weak, which is favorable for shale gas preservation.

Comprehensive preservation conditions after transformation, adjustment, and loss

The pressure coefficient and gas content are the critical parameters of the preservation conditions after transformation, adjustment, and loss of reservoir (Dong et al. 2018; Akrout et al. 2021). Wide variations are observed in the pressure coefficient of the Longmaxi reservoir in the study area (Fig. 10a). The highest pressure coefficient is greater than 2.0 with the best comprehensive preservation conditions in the northeast corner of the study area, followed by the Luochang syncline and Jianwu syncline with pressure coefficients higher than 1.6 (especially the Jianwu syncline with pressure coefficient higher than 2.0). Those are overpressure reservoirs with excellent preservation conditions. Comparatively, the Changning anticline is close to the erosion area of the Longmaxi shale, and the southwest corner is close to the erosion areas of the Junlian County and Yanjin County. As a result, the pressure coefficient gradually decreases, and most of them

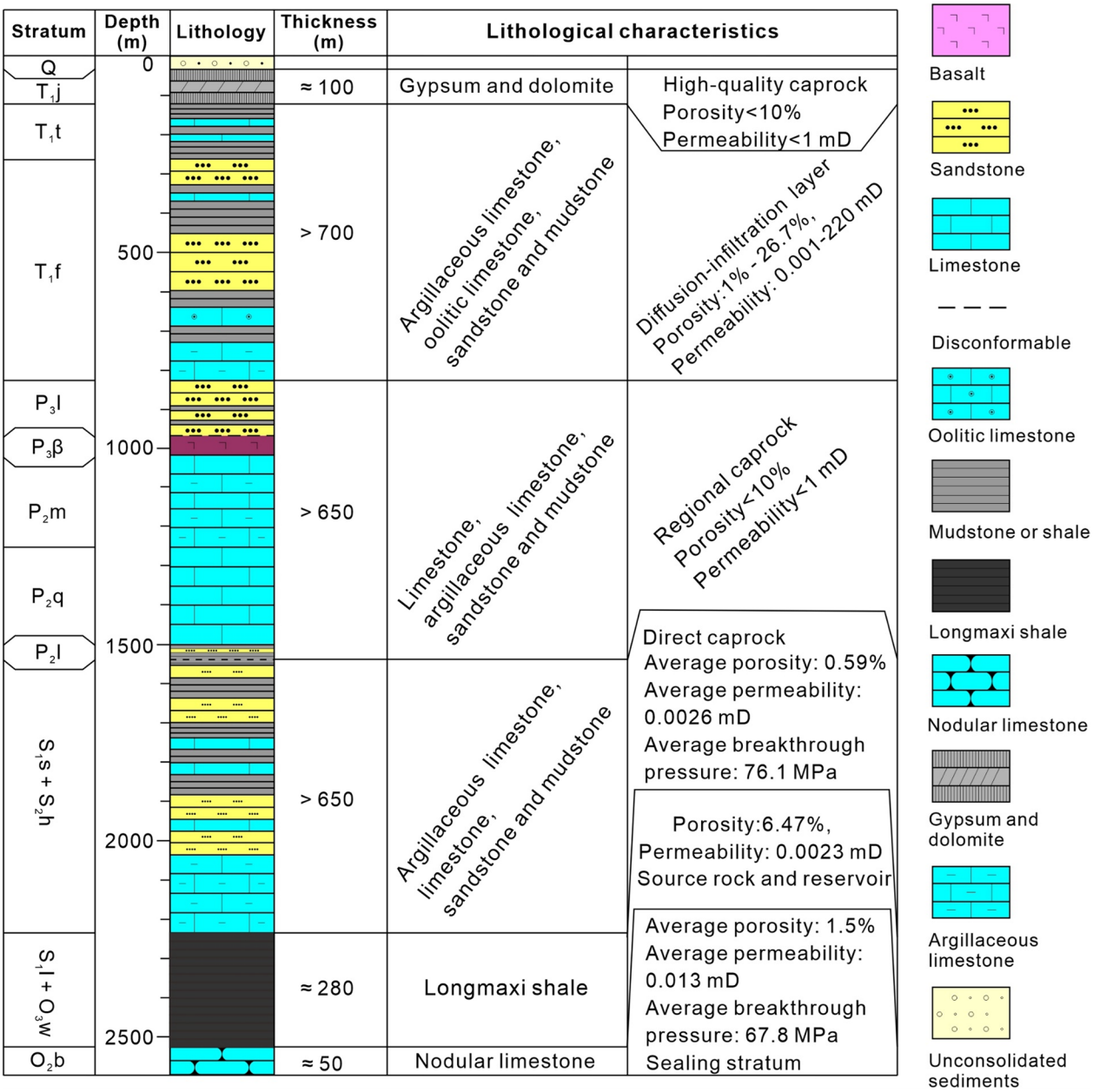

Fig. 7 Lithological characteristics and sealing ability of the strata in Well GX-1. Q is Quaternary; T_1j, T_1t, and T_1f are the Jialingjiang, Tongjiezi, and Feixianguan formations of the Lower Triassic; P_3l and $P_3\beta$ are the Leping formation and Emeishan Basalt of the Upper Permian; P_2m, P_2q, and P_2l are the Maokou, Qixia, and Liangshan formations of the Middle Permian; S_1s and S_2h are the Shiniulan and Hanjiadian formations of Lower and Middle Silurian; S_1l and O_3w are the Longmaxi and Wufeng formations of the Lower Silurian and Upper Ordovician, and O_2b is the Baotao formation of the Middle Ordovician. The data of porosity, permeability, and breakthrough pressure refer to Ou et al. (2021), Wang et al. (2021), Ning (2020), and He et al. (2019b)

are normal pressure reservoirs, or even under-pressured reservoirs with poor preservation conditions. The gas content of the reservoir refers to the sum of the lost gas, tested gas, and residual gas (Glorioso et al. 2014; Jiang et al. 2020). Except for the Changning anticline, the gas content is generally higher than 1.8 cm^3/g. The northern part of the study area has the highest gas content, ranging from 2.0 cm^3/g to 2.5 cm^3/g. In contrast, its value in the central-southern part of the study area is relatively stable, with a gas content of 1.8 cm^3/g to 2.0 cm^3/g (Fig. 10b).

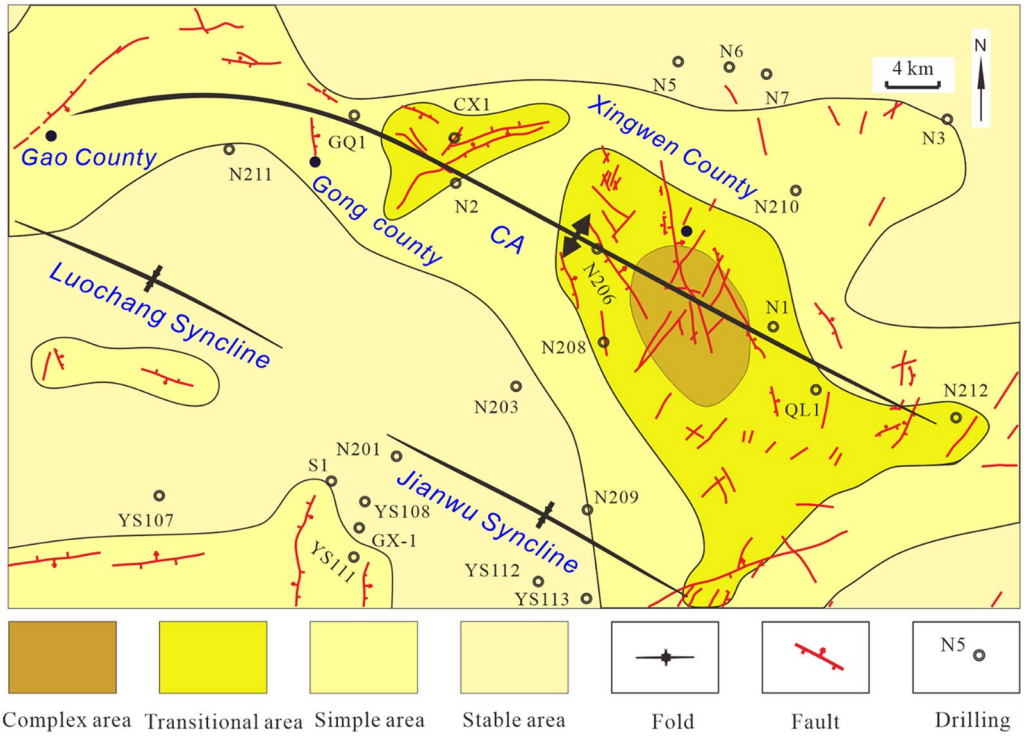

Fig. 8 Quantitative evaluation of faults in the study area. CA is the Changning Anticline

Evaluation results of reservoir quality

The reservoir grade evaluation scheme is established above, and the system's parameters are determined. Furthermore, the reservoirs are quantitatively evaluated in the study area (Fig. 11). The Gong County, Shuanghe, Meidong, and Xingwen County areas are at the core of the Changning anticline. Those are erosion and shallow burial areas of the Longmaxi shale with a burial depth less than 1000 m and a short distance from the erosion area (Fig. 6). Additionally, faults developed, caprocks are seriously damaged, and the pressure coefficient and gas content are low in those areas (Figs. 7, 8, 10). Thus, the preservation condition is poor and classified as a Non-economic area (the white area in Fig. 11). The annular area around the core of the Changning anticline and the south of the study area are classified as Class II (the yellowish-green area in Fig. 11) with the characteristics of moderate burial depth (1000–2500 m), transitional fault complexity, high-quality regional caprocks of the Shiniulan–Hanjiadian formations developed, and normal pressure–overpressure conditions (1.0–1.6) (Figs. 7, 8, 10). Areas in the Luochang syncline, Jianwu syncline, and the northeast limb of the Changning anticline are divided as Class I (the green area in Fig. 11) with the characteristics of moderate burial depth (2500–3000 m), simple-transitional fault complexity, high-quality regional caprocks of the Shiniulan–Hanjiadian and the Jialingjiang formations developed, and high pressure coefficient (1.0–2.0) and gas content (1.8–2.0 cm^3/g) (Figs. 7, 8 and 10). In addition, the northeast corner of the study area is assigned as Class III (the light green area in Fig. 11) with the characteristics of high-quality regional caprocks of the Shiniulan–Hanjiadian and the Jialingjiang formations developed, pressure coefficient over 2.0, and gas content greater than 2.0 cm^3/g, which has optimum preservation conditions, whereas the burial depth is over 3500 m, or even greater than 4500 m. Therefore, it is difficult to economically and efficiently develop this area using current engineering techniques. In general, this area has high development potential, and would be one of the commercial areas in the future with constant progress in shale gas drilling and fracturing techniques.

Formation and evolution of overpressured reservoirs

Pressure coefficient is a comprehensive characterization of the sealing capacity of reservoir and caprocks and the preservation conditions of the gas reservoir after uplift and erosion caused by tectonic uplift (Gao et al. 2019; Hua et al. 2021). The above sections also indicate that gas reservoirs with high exploration and development potential are mostly in overpressure areas (Figs. 10a and 11). Additionally, exploration and development activities also confirm that the high production gas reservoirs in Sichuan Basin are characterized by overpressure, whereas

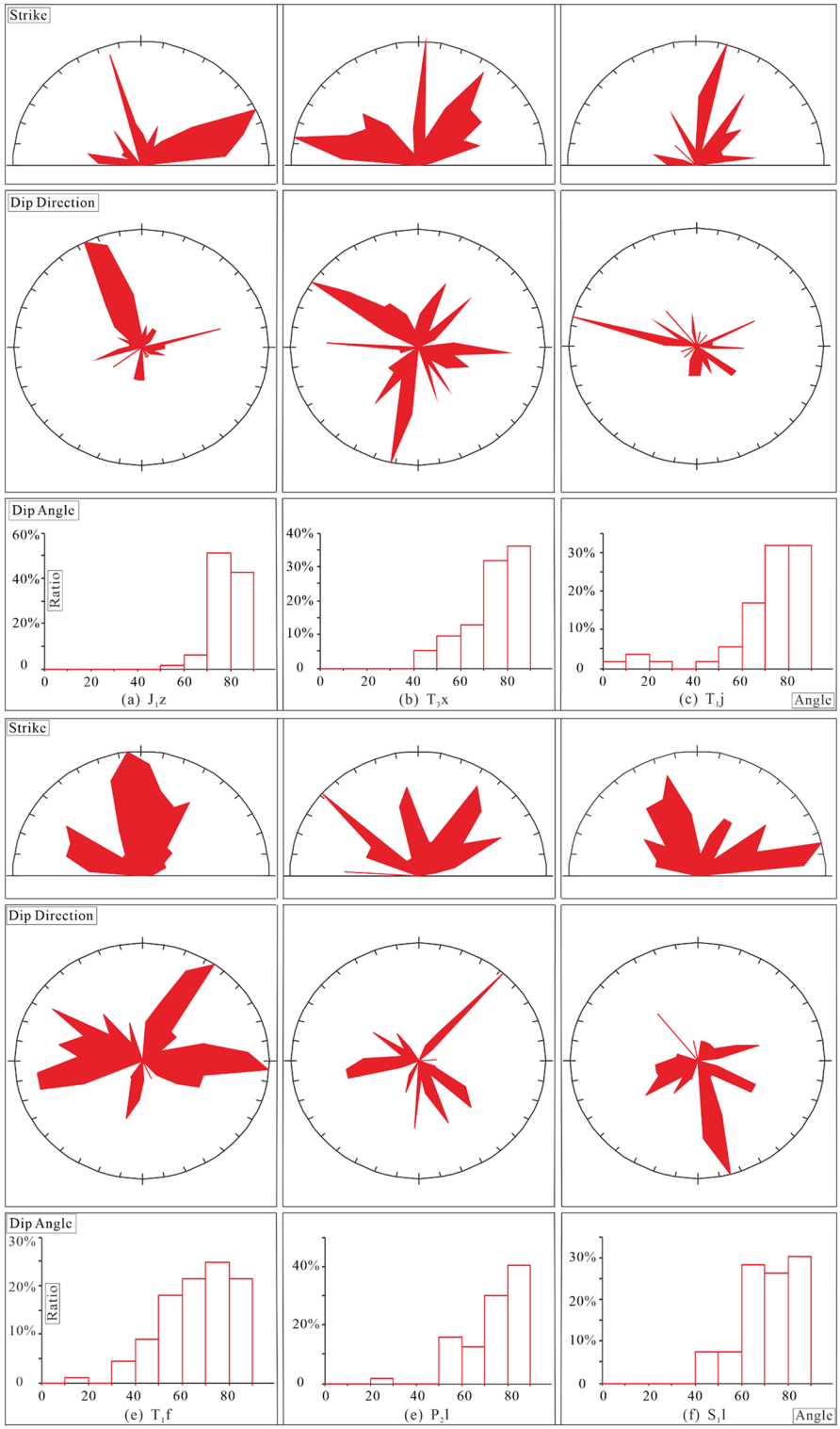

Fig. 9 The occurrence characteristics of joint points in different strata in the study area. J_1z is the Ziliujing formation of the Lower Jurassic, T_3x, T_1j and T_1f are the Xujiahe, Jialingjiang, and Feixianguan formations of the Upper and Lower Triassic, P_2l is the Leping formation of the Upper Permian, and S_1l is the Longmaxi formation of the Lower Silurian

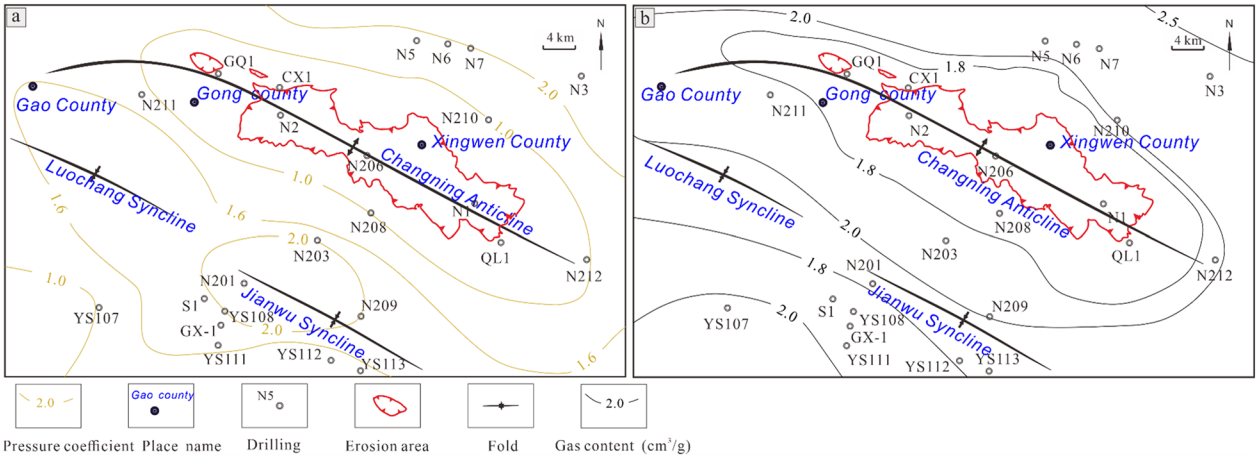

Fig. 10 Pressure coefficient (**a**) and gas content (**b**) contours of the study area (part of the data refers to Hu et al. (2014), Zhang (2018), and Liang (2018)). CA is the Changning Anticline

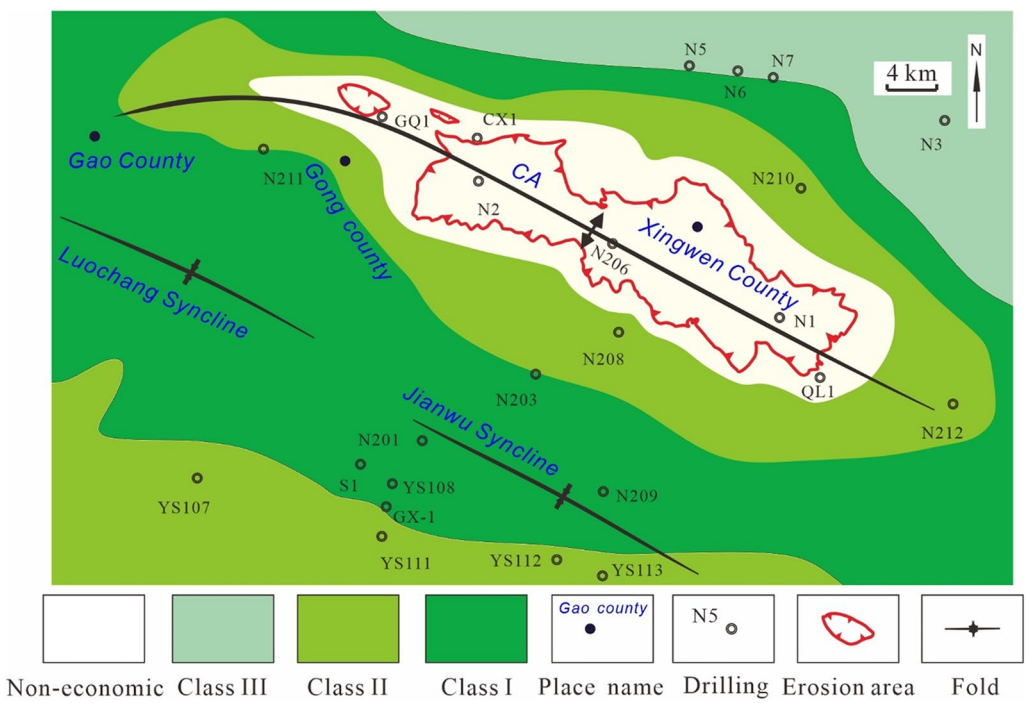

Fig. 11 Exploitation potential evaluation of the Longmaxi shale gas reservoir in the study area CA is the Changning Anticline

the production of normal-pressured reservoirs is relatively poor (Li et al. 2016; Feng et al. 2018). Consequently, the formation and evolution process of overpressured reservoir is reconstructed based on the sedimentary burial and hydrocarbon generation history of Well GX-1, and tectonic evolution and corresponding regional stress field of the southern Sichuan Basin (Fig. 12). Furthermore, the formation and preservation of overpressured reservoirs are summarized as hydrocarbon generation pressurization of organic matter, transformation dehydration pressurization of clay minerals, tectonic uplift pressurization, and maintenance of overpressure.

Hydrocarbon generation pressurization of the maturation of organic matter

Hydrocarbon generation pressurization of the maturation organic matter refers to the conversion of high-density organic matter into low-density hydrocarbon fluid as

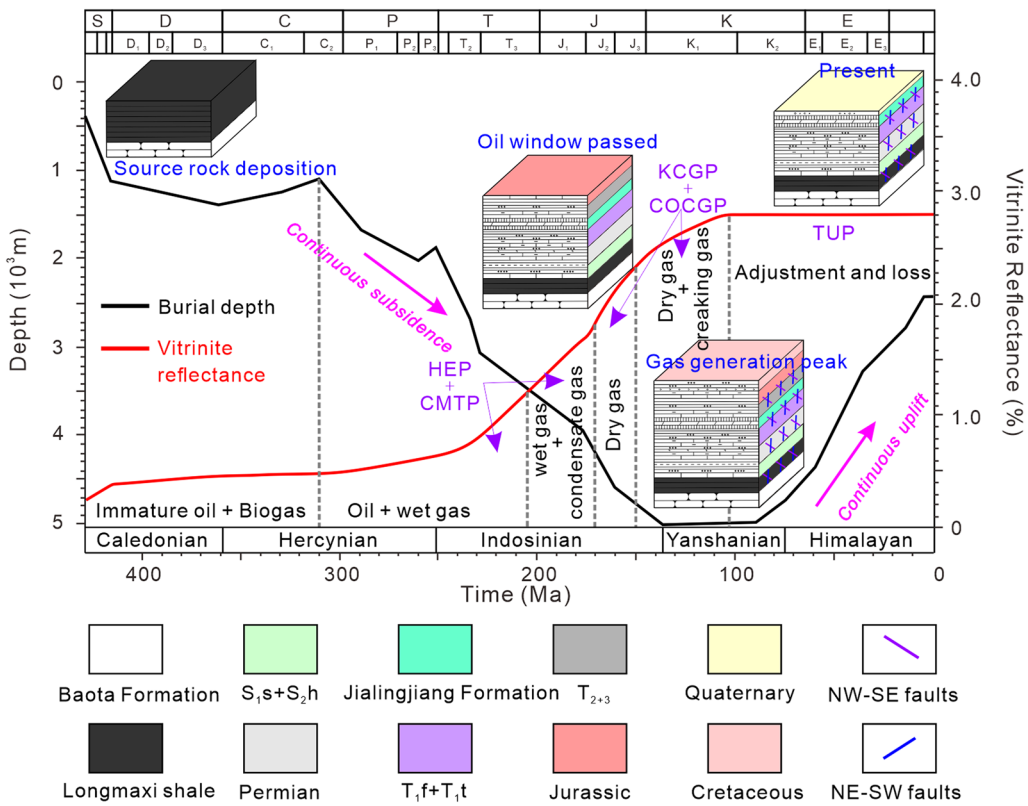

Fig. 12 Dynamic evolution process of shale gas generation, accumulation, adjustment, loss, and the formation and evolution of overpressure in Well GX-1. HEP is hydrocarbon expansion pressurization, CMTP is clay mineral transformation pressurization, KCGP is kerogen cracking gas pressurization, COCGP is crude oil cracking gas pressurization, and TUP is tectonic uplift pressurization. T_1f and T_1t are the Feixianguan and Tongjiezi formations of the Lower Triassic, T_{2+3} in the Middle and Upper Triassic, and S_1s and S_2h are Shiniulan and Hanjiadian formations of the Lower and Middle Silurian

a result of thermal evolution. This process would partially transfer the overlying formation pressure to the newly added pore-fracture fluid, resulting in microporous overpressure (Osborne and Swarbrick 1997; Ramdhan and Goulty 2010). The hydrocarbon generation pressurization is divided into several stages, from the formation of the reservoir to present time, and each stage's pressurization magnitude is significantly different (Fig. 12). (i) The primary hydrocarbon generation of organic matter formed a small amount of immature oil and biogas during the Early Silurian to Upper Carboniferous. Its contribution to the overpressured reservoir was weak due to the limitation of hydrocarbon quantity. (ii) Organic matter evolved to a "liquid window" and a large quantity of oil and wet gas generated during Upper Carboniferous to the end of the Triassic, which has a certain contribution to the reservoir pressurization due to the hydrocarbon fluid expansion. (iii) The wet gas and condensate gas were the main products at the end of Triassic to Middle Jurassic, and the influence of this process on reservoir pressurization was greater than (i) and (ii) due to the hydrocarbon quantity and the phase transition of hydrocarbon. (iv) The gas generation peak was reached (including thermal degradation gas from kerogen and pyrolysis gas from crude oil) during the Middle Jurassic to Early Cretaceous, which led to a rapid reservoir pressure increase, and its contribution was higher than (i), (ii), and (iii).

The pressurization process of hydrocarbon generation has a clear influence on the pore morphology, especially the organic matter pores. Gas overpressure in pores could offset the mechanical compaction effect of overlying sediment to a certain extent and preserve the pore space of the reservoir well. The pore morphology is predominantly elliptical to circular, and there is a pronounced directionality in the long length distribution of the pores (Fig. 5a, b, f), which indicates that the pores have suffered directional stress. The elliptical shape is the result of the coupling effect of microporous overpressure and the compressive stress of overlying strata. In comparison, Wang et al. (2020) and Peng et al. (2020) suggested that the organic matter pores in non-overpressure reservoirs have a mostly flat and irregular angular shape,

and the phenomenon of microporous overpressure is not apparent. Therefore, the pores are not well preserved, leading to low productivity. Microporous overpressure is a crucial preservation form of hydrocarbon generation pressurization of organic matter. Also, it is the basis of the formation of an overpressured reservoir.

Pressurization by clay mineral transformation and dehydration

The overpressure of the reservoir caused by the transformation and dehydration of clay minerals refers to desorption of bound water in clay particles and migration to the pores among clay particles during transformation of smectite to illite or chlorite, during the diagenetic evolution of the reservoir with greater burial depth (Audet 1995; Tanikawa et al. 2008). The released interlayer water cannot be discharged in time, resulting in abnormal high pressure of the reservoir. Clay minerals are layered silicate minerals that contain interlayer water to varying degrees, in which smectite contains the most water (four or more water molecular layers), accounting for about 23% of the weight of the mineral (Xie et al. 2022b). In the samples of this work, clay minerals consist mainly of illite (average content greater than 75%) and illite/smectite (average content greater than 20%). The average content of chlorite is less than 3%, and there is no chlorite/smectite (Table 2). Consequently, this work mainly discusses the reservoir overpressure caused by the smectite–mixed I/S–illite transformation sequence (Fig. 12). (i) Longmaxi shale was in the early diagenetic stage from the Silurian to Upper Carboniferous, and smectite began to transform into mixed I/S, the mixed layer ratio of smectite was higher than 50%. The interlayer water was discharged except for the reciprocal first and second layers, which significantly contributed to reservoir overpressure. (ii) Longmaxi shale was in the middle diagenetic stage from the Upper Carboniferous to the end of the Triassic. Smectite transformed to illite in large quantities. The mixed layer ratio of smectite was higher than 15%, and the interlayer water was discharged, except for the penultimate layer (Keller 1962). The contribution of this stage to reservoir overpressure was also significant. (iii) The Longmaxi shale was in the late diagenetic stage from the Middle Jurassic to Early Cretaceous, and the last interlayer water was removed from smectite in this stage. The impact of this process on reservoir overpressure is weaker than that in (i) and (ii). In general, clay mineral transformation has an important contribution to the overpressure of shale reservoirs, but its contribution is much weaker than the overpressure caused by hydrocarbon generation from organic matter considering the discharge period and volume of water molecules (Osborne and Swarbrick 1997; Li et al. 2016).

Tectonic uplift pressurization and maintenance of overpressure

Tectonic uplift pressurization refers to the fluid pressure in the reservoir pores that is maintained at a certain level under the tectonic uplift of the formed gas reservoir, resulting in a reservoir pressure higher than the hydrostatic pressure (Loucks and Ruppel 2007; Hill et al. 2007). Longmaxi shale gas reservoir in the study area undergoes an uplift stage from the Early Cretaceous. The temperature and pressure of the reservoir decrease, so the prominent hydrocarbon generation stops, and the transformation and dehydration of clay minerals no longer occur. Tectonic uplift is the controlling factor of reservoir overpressure preservation, consisting of tectonic uplift pressurization and damaging trap conditions leading to reservoir pressure relief. The uplift magnitude of the Longmaxi shale is greater than 2500 m near the Well GX-1 since the Early Cretaceous (Fig. 12).

In contrast, the Longmaxi shale in the core of the Changning anticline has been uplifted severely or is even absent. As a result, the pressure coefficients of gas reservoirs are quite different in the study area; namely, shallow burial depth, caprock erosion, and fault development caused by tectonic uplift control the current reservoir pressure. The integrity of the overpressured area remains relatively unaffected, the uplift magnitude is relatively small, and fault development is weak. Two sets of high-quality caprocks of the Shiniulan–Hanjiadian, and Jialingjiang formations are well preserved. As a result, a complete lithologic-structural trap remains. Comparatively, normal pressured areas are characterized by a strong tectonic disturbance, major uplift, developed gas conducting faults, lack of high-quality caprocks, and proximity to the erosion area of the Longmaxi shale (Fig. 12).

Conclusion

(1) Longmaxi shale reaches its peak gas generation in the study area during the Middle Jurassic to Early Cretaceous, and then tectonic uplift. The gas reservoir is divided into four grades of Class I, Class II, Class III, and Non-economic class based on preservation and development engineering conditions. Regions of the Jianwu–Luochang syncline and the northeast limb of the Changning anticline are regarded as the optimum reservoir (Class I). The gas reservoir in the core of the Changning anticline has the worst development potential, which is a Non-economic class. The northeast corner of the study area has excellent preservation conditions, but it is too deep and difficult to develop, classified as a Class III gas reservoir. The remaining areas

have moderate preservation and development conditions and are classified as Class II.

(2) Gas reservoirs with excellent preservation conditions are often characterized by overpressure. The formation and preservation of overpressured reservoirs are divided into the process of hydrocarbon generation pressurization of the maturation of organic matter, pressurization of clay mineral transformation and dehydration, tectonic uplift pressurization, and maintenance of overpressure. Hydrocarbon generation pressurization mainly occurs during the Upper Carboniferous to Early Cretaceous, especially during Middle Jurassic to Early Cretaceous. Transformation dehydration pressurization of clay minerals mainly occurs during the Silurian to the end of Triassic. Tectonic uplift pressurization has occurred since the Early Cretaceous. The difference in preservation conditions of shale gas reservoirs after tectonic uplift in the study area leads to the difference in the current pressure coefficient.

Supplementary Information

The online version contains supplementary material available at https://doi.org/10.1186/s40562-023-00290-x.

Additional file 1: Table S1. Basic data for recovery of burial history recovery of the Longmaxi formation in Well GX-1. The setting of sedimentary period and erosion period refers to Tang (2018). **Table S2.** Simulation boundary conditions of thermal evolution history of the Longmaxi formation in Well GX-1

Author contributions

Software, WX; writing—review and editing, WX, HG, MW, SC, VV, and HW.

Funding

The authors gratefully acknowledge the supports of the Fundamental Research Funds for National Universities, China University of Geosciences (Wuhan), Open Fund of the Key Laboratory of Tectonics and Petroleum Resources of Ministry of Education (TPR-2022-16) and China Scholarship Council.

Availability of data and materials

The data will be available on request.

Declarations

Competing interests

The authors declared that they have no conflicts of interest in this work.

Author details

[1]Key Laboratory of Tectonics and Petroleum Resources of Ministry of Education, China University of Geosciences, Wuhan 430074, China. [2]School of Earth Resources, China University of Geosciences, Wuhan 430074, China. [3]Department of Materials Engineering, KU Leuven, Campus Bruges, 8200 Brugge, Belgium. [4]Key Laboratory of Coalbed Methane Resources and Accumulation Process, Ministry of Education, China University of Mining and Technology, Xuzhou 221008, China.

Received: 26 April 2023 Accepted: 19 July 2023
Published online: 05 August 2023

References

Ahmad F, Quasim MA, Ahmad AHM (2021) Microfacies and diagenetic overprints in the limestones of middle Jurassic Fort Member (Jaisalmer formation), Western Rajasthan, India: implications for the depositional environment, cyclicity, and reservoir quality. Geol J 56(1):130–151. https://doi.org/10.1002/gj.3945

Akrout D, Ahmadi R, Mercier E et al (2021) Present-day overpressure in southern Tunisia: characterization, possible causes and implications for drilling operations. J Afr Earth Sci 184:104356. https://doi.org/10.1016/j.jafrearsci.2021.104356

Audet DM (1995) Mathematical modelling of gravitational compaction and clay dehydration in thick sediment layers. Geophys J Int 122(1):283–298. https://doi.org/10.1111/j.1365-246X.1995.tb03554.x

Chen J (2014) Shale gas preservation conditions in South Anhui of lower Yangtze area. advanced materials research. Trans Tech Publ Ltd 998:1458–1461. https://doi.org/10.4028/www.scientific.net/AMR.998-999.1458

Chen C (2018) Research on paleoceanography, paleoclimate and formation mechanism of source rock during geologic transition period from late Ordovician to early Silurian in Southern Sichuan province—Northern Guizhou province, South China. China University of Geosciences, Wuhan

Chen J, Yang S, Li H, Zhang B, Lv J (2013) Research on geographical environment unit division based on the method of natural breaks (Jenks). Int Arch Photogramm Remote Sens Spat Inf Sci 3:47–50

Chen F, Lu S, Ding X, Zhao H, Ju Y (2018) Total porosity measured for shale gas reservoir samples: a case from the lower Silurian Longmaxi formation in southeast Chongqing, China. Minerals 9(1):5. https://doi.org/10.3390/min9010005

Dong D, Shi Z, Guan Q, Jiang S, Zhang M, Zhang C, Wang S, Sun S, Yu R, Liu D, Peng P, Wang S (2018) Progress, challenges and prospects of shale gas exploration in the Wufeng-Longmaxi reservoirs in the Sichuan Basin. Nat Gas Ind B 5(5):415–424. https://doi.org/10.1016/j.ngib.2018.04.011

Feng W, Wang F, Guan J, Zhou J, Wei F, Dong W, Xu Y (2018) Geologic structure controls on initial productions of lower Silurian Longmaxi shale in south China. Mar Pet Geol 91:163–178. https://doi.org/10.1016/j.marpetgeo.2018.01.001

Freeman CM, Moridis GJ, Blasingame TA (2011) A numerical study of microscale flow behavior in tight gas and shale gas reservoir systems. Transp Porous Media 90(1):253–268. https://doi.org/10.1007/s11242-011-9761-6

Gao J, Zhang JK, He S, Zhao J, He Z, Wo Y, Feng Y, Li W (2019) Overpressure generation and evolution in lower paleozoic gas shales of the Jiaoshiba region, China: implications for shale gas accumulation. Mar Pet Geol 102:844–859. https://doi.org/10.1016/j.marpetgeo.2019.01.032

Ge X, Hu W, Ma Y, Li M, Tang J, Zhao P (2021) Quantitative evaluation of geological conditions for shale gas preservation based on vertical and lateral constraints in the Songkan area, Northern Guizhou, southern China. Mar Pet Geol 124:104787. https://doi.org/10.1016/j.marpetgeo.2020.104787

Glorioso JC, Rattia A, Lolley R (2014) A review of the fundamentals of shale gas evaluations: the dangers of effective porosity and clay excess conductivity corrections. In SPE/EAGE European Unconventional Resources Conference and Exhibition. European Association of Geoscientists & Engineers. 2014(1) 1–9 https://doi.org/10.2118/167785-MS

Guo T (2016) Key geological issues and main controls on accumulation and enrichment of Chinese shale gas. Pet Explor Dev 43(3):349–359. https://doi.org/10.1016/S1876-3804(16)30042-8

Han S, Zhang J, Yang C, Bai S, Huang L, Dang W, Wang C (2016) Well log evaluation of shale gas reservoirs and preservation conditions of lower Cambrian shale succession in Cengong Block of southeast Sichuan basin, south China. J Nat Gas Sci Eng 33:337–346. https://doi.org/10.1016/j.jngse.2016.05.019

He D, Lu R, Huang H, Wang X, Jiang H, Zhang W (2019a) Tectonic and geological setting of the earthquake hazards in the Changning shale gas development zone, Sichuan Basin SW China. Pet Explor Dev 46(5):1051–1064. https://doi.org/10.1016/S1876-3804(19)60262-4

He S, Qin Q, Fan C, Zhou J, Wei Z, Huang W (2019b) Shale gas preservation conditions in Dingshan area, Southeastern Sichuan. Pet Geol Recover Eff 26(2):24–31

Hill RJ, Zhang E, Katz BJ, Tang Y (2007) Modeling of gas generation from the barnett shale, Fort Worth Basin Texas. AAPG Bull 91(4):501–521. https://doi.org/10.1306/12060606063

Hu D, Zhang H, Ni K, Yu C (2014) Main controlling factors for gas preservation conditions of marine shales in southeastern margins of the Sichuan Basin.

Nat Gas Ind 34(6):17–23. https://doi.org/10.3787/j.issn.1000-0976.2014.06.003
Hua Y, Guo X, Tao Z, He S, Dong T, Han Y, Yang R (2021) Mechanisms for overpressure generation in the bonan sag of Zhanhua depression, Bohai Bay Basin China. Mar Pet Geol 128:105032. https://doi.org/10.1016/j.marpetgeo.2021.105032
Ibrahim Mohamed M, Salah M, Coskuner Y, Ibrahim M, Pieprzica C, Ozkan E (2019) Integrated approach to evaluate rock brittleness and fracability for hydraulic fracturing optimization in shale gas in SPE Oklahoma city oil and gas Symposium. OnePetro. https://doi.org/10.2118/195196-MS
Jarvie DM, Hill RJ, Ruble TE, Pollastro RM (2007) Unconventional shale-gas systems: the mississippian barnett shale of north-central Texas as one model for thermogenic shale-gas assessment. AAPG Bull 91(4):475–499. https://doi.org/10.1306/12190606068
Jiang Q, Zhu C, Qiu N, Cao H (2015) Paleo-heat flow and thermal evolution of the lower Cambrian Qiongzhusi shale in the southern Sichuan Basin SW China. Nat Gas Geosci 26(8):1563–1570
Jiang Y, Fu Y, Xie J, Dong D, Zhou K, Cheng X, Qi L, Zhang H, Chen C, Ma T, Gu Y (2020) Development trend of marine shale gas reservoir evaluation and a suitable comprehensive evaluation system. Nat Gas Ind B 7(3):205–214. https://doi.org/10.1016/j.ngib.2019.10.003
Jin X, Shah SN, Roegiers JC, Zhang B (2014) Fracability evaluation in shale reservoirs-an integrated petrophysics and geomechanics approach. In SPE hydraulic fracturing technology conference, 4–6 February. OnePetro. SPE-168589-MS. https://doi.org/10.2118/168589-MS
Keller WD (1962) Diagenesis in clay minerals—A review. Clays Clay Miner 11(1):136–157
Kirk MF, Martini AM, Breecker DO, Colman DR, Takacs-Vesbach C, Petsch ST (2012) Impact of commercial natural gas production on geochemistry and microbiology in a shale-gas reservoir. Chem Geol 332:15–25. https://doi.org/10.1016/j.chemgeo.2012.08.032
Li J (2012) Study on evaluation system of marine shale gas in South China. Northwest University, Xi'an
Li S, Yuan Y, Sun W, Sun D, Jin Z (2016) Formation and destruction mechanism as well as major controlling factors of the silurian shale gas overpressure in the Sichuan Basin China. J Nat Gas Geosci 1(4):287–294. https://doi.org/10.1016/j.jnggs.2016.09.002
Li W, Yu Z, Wang X, Yu Z, Lu X, Feng Q (2020) Formation mechanisms of deep and ultra-deep over pressure caprocks and their relationships with super-large gas fields in the petroliferous basins of China. Nat Gas Industry B 7(5):443–452. https://doi.org/10.1016/j.ngib.2020.09.002
Liang F (2018) The research on shale gas enrichment pattern and the favorable area optimizing of Wufeng- Longmaxi shale in middle and upper Yangtze region. China University of Mining and Technology, Xuzhou
Liao W (2019) Wufeng formation-Longmaxi formation shale gas preservation condition analysis in Huolongping—Sangzheping Syncline, Xianfeng County Hubei Province. Coal Geol China 31(S1):22–27
Liu B, Lv Y, Zhao R, Tu X, Guo X, Shen Y (2012) Formation overpressure and shale oil enrichment in the shale system of Lucaogou formation, Malang Sag, Santanghu Basin NW China. Pet Explor Dev 39(6):744–750. https://doi.org/10.1016/S1876-3804(12)60099-8
Liu W, Zhou X, Xu X, Zhang S (2020) Formation of inter-salt overpressure fractures and their significances to shale oil and gas: a case study of the third member of Paleogene Shahejie formation in Dongpu sag, Bohai Bay Basin. Pet Explor Dev 47(3):560–571. https://doi.org/10.1016/S1876-3804(20)60073-8
Loucks RG, Ruppel SC (2007) Mississippian Barnett Shale: lithofacies and depositional setting of a deepwater shale-gas succession in the Fort Worth Basin, Texas. AAPG Bull 91(4):579–601. https://doi.org/10.1306/11020606059
Loucks RG, Reed RM, Ruppel SC, Hammes U (2012) Spectrum of pore types and networks in mudrocks and a descriptive classification for matrix-related mudrock pores. AAPG Bull 96(6):1071–1098. https://doi.org/10.1306/08171111061
Luo Q, Zhong N, Dai N, Zhang W (2016) Graptolite-derived organic matter in the Wufeng-Longmaxi formations (upper ordovician-lower silurian) of southeastern Chongqing, China: implications for gas shale evaluation. Int J Coal Geol 153:87–98. https://doi.org/10.1016/j.coal.2015.11.014
Ma X, Li X, Liang F, Wan Y, Shi Q, Wang Y, Zhang X, Che M, Guo W, Guo W (2020a) Dominating factors on well productivity and development strategies optimization in Weiyuan shale gas play, Sichuan Basin SW China. Pet Explor Dev 47(3):594–602. https://doi.org/10.1016/S1876-3804(20)60076-3
Ma X, Xie X, Yong R, Zhu Y (2020b) Geological characteristics and high production control factors of shale gas reservoirs in Silurian Longmaxi formation, southern Sichuan Basin SW China. Pet Explor Dev 47(5):901–915. https://doi.org/10.1016/S1876-3804(20)60105-7
Magara K (1981) Static versus dynamic interpretation in petroleum geology. AAPG Bull 65(3):531–539. https://doi.org/10.1306/2F91980A-16CE-11D7-8645000102C1865D
Moridis G, Reagan M (2021) Evaluation of the effectiveness of continuous gas displacement for EOR in hydraulically fractured shale reservoirs. SPE J 26(04):2068–2091. https://doi.org/10.2118/198999-PA
Ning C (2020) Reservoir characteristics and favorable area prediction of Qixia Formation in Shuangyushi area. Chengdu, Chengdu University of Technology, North Sichuan
Osborne MJ, Swarbrick RE (1997) Mechanisms for generating overpressure in sedimentary basins: a reevaluation. AAPG Bull 81(6):1023–1041. https://doi.org/10.1306/522B49C9-1727-11D7-8645000102C1865D
Ou F, Yang H, Huang X (2021) Application of logging interpretation method for reef shoal reservoir in Feixianguan formation of X Gas Field. Reserv Eval Dev 11(5):744–752
Peng Y, Long S, He X, Tang J, Ni H, Gao Y (2020) Characteristics of normal-pressure shale gas reservoirs and evaluation of its favorable areas in Pengshui. Reserv Eval Dev 10(05):12–19
Ramdhan AM, Goulty NR (2010) Overpressure-generating mechanisms in the Peciko field, lower Kutai Basin Indonesia. Pet Geosci 16(4):367–376. https://doi.org/10.1144/1354-079309-027
Rashid F, Hussein D, Lawrence JA, Khanaqa P (2020) Characterization and impact on reservoir quality of fractures in the cretaceous Qamchuqa formation, Zagros folded belt. Mar Pet Geol 113:104117. https://doi.org/10.1016/j.marpetgeo.2019.104117
Rodrigues AG, Goldberg K (2014) Primary composition and diagenetic patterns of sandstones from Barra de Itiúba formation in atalaia high, Sergipe Sub-Basin Brazilian. J Geol 44:545–560. https://doi.org/10.5327/Z2317-4889201400040003
Rouquerol J, Avnir D, Fairbridge CW, Everett DH, Haynes JM, Pernicone N, Ramsay JDF, Sing KSW, Unger KK (1994) Recommendations for the characterization of porous solids (Technical Report). Pure Appl Chem 66(8):1739–1758. https://doi.org/10.1351/pac199466081739
Shoieb MA, Sum CW, Ismail MS, Gebretsadik HT, Esther O (2020) Geological field characteristic of the Kroh formation in the Upper Perak shales, western Peninsula Malaysia. J Nat Gas Geosci 5(1):29–32. https://doi.org/10.1016/j.jnggs.2019.11.005
Tang X (2018) Tectonic control of shale gas accumulation in Longmaxi formation in the southern Sichuan Basin. China University of Mining and Technology, Xuzhou, XuZhou
Tang X, Jiang S, Jiang Z, Li Z, He Z, Long S, Zhu D (2019) Heterogeneity of paleozoic Wufeng-Longmaxi formation shale and its effects on the shale gas accumulation in the upper yangtze Region, China. Fuel 239:387–402. https://doi.org/10.1016/j.fuel.2018.11.022
Tanikawa W, Shimamoto T, Wey SK, Lin CW, Lai WC (2008) Stratigraphic variation of transport properties and overpressure development in the western foothills Taiwan. J Geophys Res: Solid Earth 113:B12403. https://doi.org/10.1029/2008JB005647
Tu Y, Zou H, Meng H, Xia Z, Nan L (2014) Evaluation criteria and classification of shale gas reservoirs. Oil Gas Geol 35(1):153–158. https://doi.org/10.11743/ogg20140120
Ukaomah CF, Zhang L, Xu Y, Sun M, Yang B, Madaki AI, Umeobi HI, Aminu MD (2021) Pore structure and seal capacity of Ilaro formation shales in the eastern Dahomey Basin: implications from mercury injection capillary pressure and spontaneous imbibition analyses. Energy Fuels 35(12):10086–10101. https://doi.org/10.1021/acs.energyfuels.1c01153
Wang M, Xie W, Huang K, Dai X (2019) Fine characterization of lithofacies and pore network structure of continental shale: case study of the Shuinan formation in the north Jiaolai Basin, China. J Petrol Sci Eng 175:948–960. https://doi.org/10.1016/j.petrol.2019.01.011
Wang R, Nie H, Hu Z, Liu G, Xi B, Liu W (2020) Controlling effect of pressure evolution on shale gas reservoirs: a case study of the Wufeng-Longmaxi formation in the Sichuan Basin. Nat Gas Ind 40(10):1–11
Wang S, Peng Y, Xiao G, Yang Z, Qianyang J, Liu Q (2021) Sedimentary facies and reservoir characteristics of Jialingjiang formation in Puguang area.

Pet Geol Eng 35(1):8-14 21. https://doi.org/10.3969/j.issn.1673-8217.2021.01.003
Wilson TH, Hart AK, Sullivan P (2016) Interrelationships of marcellus shale gas production to frac-induced microseismicity, interpreted minor faults and fractures zones, and stimulated reservoir volume, Greene County Pennsylvania. Interpretation 4(1):T15–T30
Xie W, Wang M, Wang X, Wang Y, Hu C (2021) Nano-pore structure and fractal characteristics of shale gas reservoirs: a case study of Longmaxi formation in southeastern Chongqing China. J Nanosci Nanotechnol 21(1):343–353. https://doi.org/10.1166/jnn.2021.18721
Xie W, Gan H, Chen C, Vandeginste V, Chen S, Wang M, Wang J, Yu Z (2022a) A model for superimposed coalbed methane, shale gas and tight sandstone reservoirs, Taiyuan formation, Yushe-Wuxiang block, eastern Qinshui basin. Sci Rep 12(1):1–15
Xie W, Chen S, Vandeginste V, Yu Z, Wang H, Wang M (2022b) Review of the effect of diagenetic evolution of shale reservoir on the pore structure and adsorption capacity of clay minerals. Energy Fuels 36(9):4728–4745. https://doi.org/10.1021/acs.energyfuels.2c00675
Xu H, Zhou W, Hu Q, Yi T, Ke J, Zhan A, Lei Z, Yu Y (2021) Quartz types, silica sources and their implications for porosity evolution and rock mechanics in the paleozoic Longmaxi formation shale Sichuan Basin. Mar Pet Geol 128:105036. https://doi.org/10.1016/j.marpetgeo.2021.105036
Yang Y (2016) Study on shale reservoir of the Longmaxi formation of lower silurian in changning area, Southern Sichuan. Southwest Petroleum University, Chengdu
Yasin Q, Baklouti S, Khalid P, Ali SH, Boateng CD, Du Q (2021) Evaluation of shale gas reservoirs in complex structural enclosures: a case study from patala formation in the kohat-potwar plateau, Pakistan. J Pet Sci Eng 198:108225. https://doi.org/10.1016/j.petrol.2020.108225
Yu W, Luo Z, Javadpour F, Varavei A, Sepehrnoori K (2014) Sensitivity analysis of hydraulic fracture geometry in shale gas reservoirs. J Pet Sci Eng 113:1–7. https://doi.org/10.1016/j.petrol.2013.12.005
Zeng X (2011) A study on shale gas of lower silurian Longmaxi formation in Sichuan basin and its peripheral areas. Chengdu University of Technology, Chengdu
Zhang X (2018) Geological characteristics of shale gas in Wufeng-Longmaxi formations of the Changning area. Southwest Petroleum university, Chengdu
Zou C, Dong D, Wang Y, Li X, Huang J, Wang S, Guan Q, Zhang C, Wang H, Liu H, Bai W, Liang F, Lin W, Zhao Q, Liu D, Yang Z, Liang P, Sun S, Qiu Z (2016) Shale gas in China: characteristics, challenges and prospects (II). Pet Explor Dev 43(2):182–196. https://doi.org/10.1016/S1876-3804(16)30022-2

Publisher's Note